Published in: Journal of Molecular Biology (2005), vol. 345, iss. 4, pp. 785-795.
Status: Postprint (Author's version)

A Metallo-β-lactamase Enzyme in Action: Crystal Structures of the Monozinc Carbapenemase CphA and its Complex with Biapenem

Gianpiero Garau[1], Carine Bebrone[2], Christine Anne[2], Moreno Galleni[2] Jean-Marie Frère[2] and Otto Dideberg[1]

[1]*Institut de Biologie Structurale Jean-Pierre Ebel (CNRS-CEA-UJF), 41, rue Jules Horowitz, F-38027 Grenoble Cedex 1, France*
[2]*Centre d'Ingenierie des Protéins, Université de Liège Sart-Tilman, B4000 Liège Belgium*

Abstract

One strategy developed by bacteria to resist the action of β-lactam antibiotics is the expression of metallo-β-lactamases. CphA from *Aeromonas hydrophila* is a member of a clinically important subclass of metallo-β-lactamases that have only one zinc ion in their active site and for which no structure is available. The crystal structures of wild-type CphA and its N220G mutant show the structural features of the active site of this enzyme, which is modeled specifically for carbapenem hydrolysis. The structure of CphA after reaction with a carbapenem substrate, biapenem, reveals that the enzyme traps a reaction intermediate in the active site. These three X-ray structures have allowed us to propose how the enzyme recognizes carbapenems and suggest a mechanistic pathway for hydrolysis of the β-lactam. This will be relevant for the design of metallo-β-lactamase inhibitors as well as of antibiotics that escape their hydrolytic activity.

Keywords: antibiotic resistance ; drug design ; enzymatic mechanism ; 3D structure ; X-ray crystallography

Abbreviations used: WT, wild-type ; r.m.s., root-mean-square ; ICP-MS, inductively coupled plasma-mass spectrometry.

Introduction

β-Lactam antibiotics have been used successfully for several decades to target the enzymes involved in the last step of peptidoglycan synthesis. Nowadays, the worldwide spread of β-lactamase-pro-ducing organisms is an important public health threat. Metallo-β-lactamases, enzymes containing approximately 230 residues, are clustered into three different subclasses, B1, B2, and B3.[1] Sequence identity ranges from 0.40-0.25 in one subclass and from 0.20-0.10 between subclasses. Subclass Bl enzymes have been found in strains of *Bacillus, Bacteroides, Pseudomonas, Serratia,* and *Chryseobacterium,* and subclass B3 enzymes have been found in strains of *Stenotrophomonas, Legionella, Fluoribacter, Janthinobacterium,* and *Caulobacter.* Both the Bl and B3 subclasses have a broad-spectrum profile (including penicillins, cephalosphorins, and carbapenems) and, *in vitro,* require two zinc ions for maximal enzymatic activity. However, metallo-β-lactamases can display different metal-binding affinities for zinc ion and, at low concentrations (picomolar range) of free zinc appear to be active with a single zinc ion per monomer.[2] Subclass B2 enzymes have a narrow substrate profile, hydro-lyzing carbapenems almost exclusively. These carbapenemases are produced by various species of *Aeromonas* and are active only in the monozinc form.[3] In contrast to the situation with serine-β-lactamases, no clinically approved metallo-β-lactamase inhibitor is available.

X-ray structures have been reported for enzymes of subclasses B1 and B3,[4-8] and all show the existence of a binuclear zinc active site. The Zn1 site is formed by a triad of histidine residues in both subclasses, whereas the Zn2 site is formed by an Asp-Cys-His triad in subclass B1 and by Asp-His-His in subclass B3. Interestingly, on the basis of sequence alignments, subclass B2 proteins have Asn-His-His and Asp-Cys-His triads for the Zn1 site and the Zn2 site, respectively.

Scheme 1. *The reaction catalyzed by the CphA enzyme.*

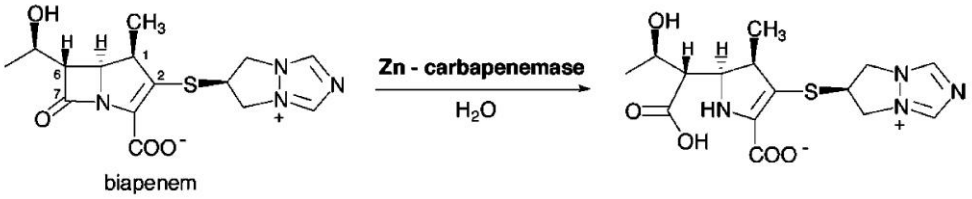

biapenem

To obtain a better understanding of the metallo-β-lactamase family and of their catalytic mechanism, we have produced the first crystal structures of the wild-type (WT) and N220G mutant forms of the subclass B2 *Aeromonas hydrophila* enzyme CphA. These structures reveal that this enzyme has a single zinc ion in the active site, located in the Zn2 site. Furthermore, by forming a complex of CphA and the antibiotic biapenem (Scheme 1), we were able to trap a reaction intermediate. This is the first crystal structure of a metallo-β-lactamase with an antibiotic molecule bound in the active site.

Results

Wild-type CphA structure

Aeromonas hydrophila CphA consists of 227 amino acid residues with a calculated molecular mass of 25.2 kDa. Since crystals of the WT CphA protein could not be obtained, ten single-site mutants were engineered by site-directed mutagenesis and overproduced. The mutants were selected in order to introduce residues that are conserved in either subclass B1 or B3, or in both. The N220G mutant crystallized in a few days, allowing us first to solve the structure of the mutant, then to grow WT crystals. The kinetic parameters of the WT and N220G mutant enzymes were not significantly different, indicating a good conservation of the WT functional properties for the mutant (Table 1). The structure of the WT protein was solved by molecular replacement using the CphA mutant structure as the starting model and was refined to a resolution of 1.7 Å. The *R*-factor and R_{free} for the refined structure were 0.19 and 0.20, respectively. The crystals adopt a $C222_1$ space group with one molecule in the asymmetric unit. The crystallographic and model statistics for the WT and N220G mutant structures, together with that for the biapenem-CphA complex, are reported in Table 2.

The model of the WT structure includes 224 amino acid residues (41-304, using the BBL numbering),[1] the catalytically essential zinc ion, one carbonate anion located in the active site, one sulphate ion, and 178 water molecules. The electron density for Pro305 (excluding the N backbone atom) and for the last two residues of the polypeptide chain was not interpretable.

CphA is a monomeric globular protein having the general αββα fold as described (Figure 1).[4] Four β-strands (β1, β2, β3, and β4), two helix-strand elements (α1β5 and α2β6), one long α-helix (α3), and the β7 strand form the N-domain, while four β-strands (β8, β9, β10, and β11) one 3_{10} helix, the α4 helix, the βl2 strand, and the α5 helix form the C-domain. The N and C-domains face each other through sheets β1-7 and β8-12. The α1 and α2 helices of the N-domain and helices α4 and α5 of the C-domain are located externally on opposite faces of the β-strand core. In contrast to all reported Bl and B3 subclass structures, a long α3 helix is located near the active-site groove. The α3 helix, formed by residues Arg140-Leu161, has a kink, which allows the helix to follow the curvature of the protein. The helix is followed immediately by an unusual proline-rich loop (Pro162, Pro165, Pro168, and Pro172). Comparison of the fold for one representative of each subclass is represented in rainbow-coloured ribbon in Figure 2. Only non-conserved secondary structures in the three subclasses are labelled to highlight structural differences in the superfamily.

Table 1. *Kinetic parameters of the wild type and selected mutants of CphA*

	Imipenem			Biapenem		
Enzyme	k_{cat} (s^{-1})	K_m (μM)	k_{cat}/K_m ($M^{-1}s^{-1}$)	k_{cat}(s^{-1})	K_m (μM)	k_{cat}/K_m ($M^{-1}s^{-1}$)
Wild-type	1200	340	3.5×10^{-6}	300	166	1.8×10^{-6}
N220G	390	50	7.8×10^{-6}	160	118	1.3×10^{-6}

S.D. values were below 10%.

Published in: Journal of Molecular Biology (2005), vol. 345, iss. 4, pp. 785-795.
Status: Postprint (Author's version)

Table 2. *Data collection, phasing and refinement statistics*

	CphA	CphA	HgMAD		CphA-biapenem
Dataset	Native	Mutant	λ_1 mutant (peak)	λ_2 mutant (edge)	Complex
A. *Data collection statistics*					
Wavelength (Å)	0.9795	0.9797	1.00783	1.01082	1.54179
Resolution (Å)[a]	23.6-1.70 (1.79-1.70)	58.9-1.60 (1.69-1.60)	58.7-1.65	58.7-1.65	26.5-1.90 (1.96-1.90)
Unique reflections	27,567	32,222	30,753	30,720	20,636
Space group	$C222_1$	$C222_1$	$C222_1$	$C222_1$	$C222_1$
Unit cell dimensions					
a (Å)	42.63	42.67	42.69	42.72	42.83
b (Å)	101.21	101.08	101.40	101.38	101.51
c (Å)	118.23	117.36	117.26	117.32	117.36
Completeness[a] (%)	94.7 (94.7)	93.1 (93.1)	96.0 (96.0)	97.0 (97.0)	99.9 (99.9)
Multiplicity[a]	3.5 (3.0)	5.8 (3.4)	6.4 (3.9)	6.3 (4.9)	5.9 (5.2)
R_{sym}[a,b] (%)	12 (31)	5 (7)	5 (8)	4 (9)	12 (29)
$I/\sigma(I)$[a]	3.9 (1.8)	8.7 (8.1)	11.1 (7.4)	12.6 (6.6)	3.7 (2.1)
B. *Phasing statistics*					
Heavy-atom sites			1	1	
FOM (centric/acentric)		0.66/0.78			
C. *Refinement statistics*					
R-factor/R_{free}[c,d] (%)	18.5/20.3	15.6/18.1			15.4/18.5
R.m.s. deviations					
Bond lengths (Å)	0.017	0.011			0.017
Bond angles (deg.)	1.63	1.36			1.75
Number of atoms					
Protein	1759	1775			1759
Zn	1x1	1x1			1x1
Carbonate	1x4	1x4			-
Biapenem	-	-			1x25
Sulphate	1x5	3x5			6x5
Glycerol	-	2x6			1x6
Water	178	258			188
Average B-factor (A^2)					
Protein	15.9	12.2			18.1
Zn	13.9	10.5			17.8
Carbonate	24.5	23.9			-
Biapenem	-	-			23.9
Sulphate	33.7	32.5			35.0
Glycerol	-	33.7			42.3
Water	23.7	23.3			26.6

[a] Numbers in parentheses are for the highest-resolution shell.
[b] $R_{sym} = \sum|I(hkl) - \langle I(hkl)\rangle|/\sum\langle I(hkl)\rangle$.
[c] *R*-factor = $\sum|F_o(hkl) - F_c(hkl)|/\sum|F_o(hkl)|$.
[d] R_{free} was calculated based on 5% of the total data omitted during structure refinement.

Published in: Journal of Molecular Biology (2005), vol. 345, iss. 4, pp. 785-795.
Status: Postprint (Author's version)

Figure 1. *Stereo view of the three-dimensional structure of the wild-type Aeromonas hydrophila CphA metallo-β-lactamase. α-Helices are shown in red, the 3_{10} helix in orange, strands in cyan, and loops in yellow. The zinc ion is represented as a green sphere. The triad of zinc ligands D120, C221, and H263, together with the carbonate ion bonded to the metal ion, are shown.*

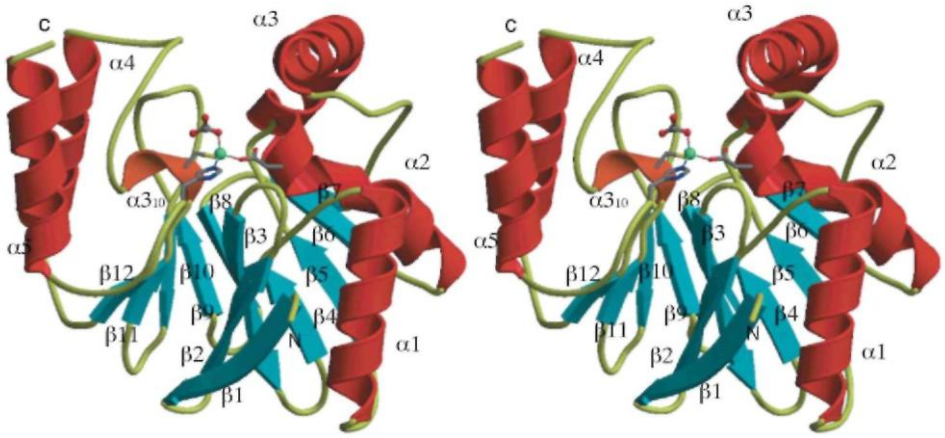

Figure 2. *Ribbon representations of the three subclasses; (a) BCII from Bacillus cereus, (b) this work and (c) FEZ-1 from Fluoribacter gormanii. The ribbon is coloured along the sequence on a residue-per-residue basis by a rainbow colour ramp. Secondary structure elements not conserved in one subclass are labelled. Zinc ions are represented as a grey sphere.*

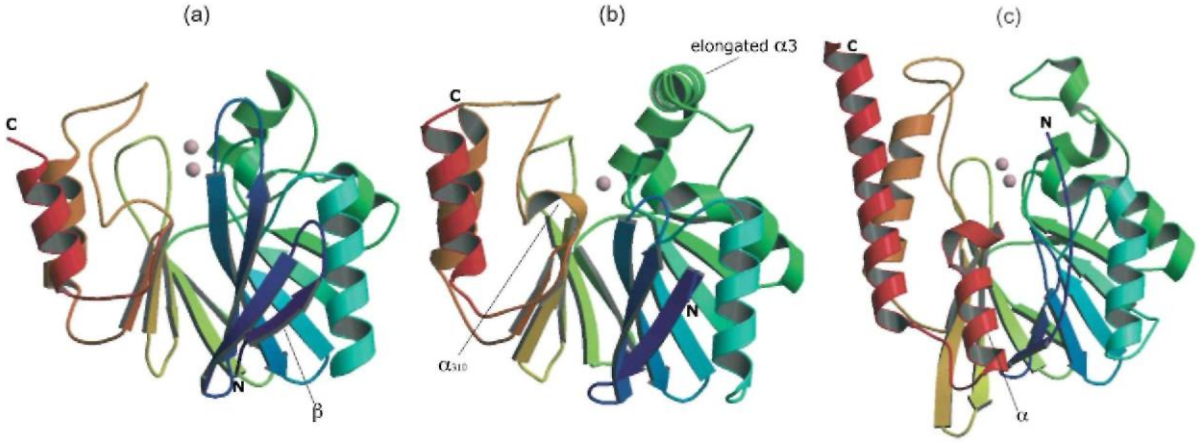

The ψ/φ angles of Tyr60, Thr86, Ala195, Asn220, and Asp264 are located in the disallowed areas of the Ramachandran plot. The last three are adjacent to an amino acid involved in one of the zinc-binding sites (Zn1 or Zn2) and, in most other sequences, are glycine residues. Tyr60 is on a loop connecting two β-strands (β2 and β3), which force Tyr60 to adopt a strained conformation (ψ = 58°; φ = -123°). Thr86 is on a loop connecting β4 to α1 and is adjacent to Trp87. A group of hydrophobic side-chains (Tyr59, Val67, Trp87, Tyr164, Pro165, and Phe236), together with other side-chains located on the α3 helix (Ile153, Phe156, and Leu161), appear to form a "hydrophobic wall", which defines the active site. Ala 195 (ψ = -160°; φ = -160°) is located on a loop between strands β8 and β9, which, at its apex, bears His196, which is involved in the active-site hydrogen bond network. Asn220 is the first residue of the 3_{10} helix and precedes the zinc-coordinating residue, Cys221, while Asp264 follows another zinc-coordinating residue, His263. Both Asn220 and Asp264 have a strained conformation of about ψ = 60° and φ = -160°. Another important residue in the CphA structure is Gly84. All available B2 subclass sequences show a glycine residue at position 84, while B1 and B3 subclass enzymes have a buried Asp (or exceptionally an Asn), which adopts a strained conformation.[8] Gly84 interrupts the β4 strand and turns the protein backbone through 90°, creating a hole inside the CphA structure that is occupied by a buried water molecule close to the Glu69 and Arg121 side-chains. The water molecule has a low *B*-factor (9 $Å^2$) and makes three hydrogen bonds: two with backbone atoms (the nitrogen atom of Thr40 and the carbonyl oxygen atom of Asp90) and one with the hydroxyl group of Ser25. Those bonds should increase the stability of the protein. In the CphA structure, there are four buried charged residues, Asp57, Glu69, Arg121, and Asp199, the first three of which lie close together. Glu69 and Arg121 form a salt-bridge, while Asp57 and Glu69 form a very short

hydrogen bond (2.5 Å), indicating the presence of a shared hydrogen atom between the two side-chains. The side-chains of Asp57 and Glu69 bridge the β2 and β3 strands, but these residues are not conserved in the other sequences. Asp199, conserved in subclasses B1 and B2, makes two hydrogen bonds with the Thrl42 and Thr197 side-chains. The importance of Arg121 and Asn220 is discussed in the following section.

Secondary structure elements bear two of the three residues involved in zinc coordination, Asp120 in the α2 helix and Cys221 in the 3_{10} helix. The third residue, His263, is located on the loop connecting β12 and β13 (Figure 1). The distances between the Zn atom and the Asp120 carboxyl oxygen atom, the Cys221 sulfur atom, and the His263 side-chain nitrogen atom are 1.96 Å, 2.20 Å, and 2.05 Å, respectively. Finally, a carbonate ion is bonded to the zinc (2.09 Å), and the four coordinating atoms, from Asp120, Cys221, His263, and O1 of CO_3^{2-}, generate a tetrahedral geometry around the metal ion.

It is interesting to note that the first reported metallo-β-lactamase structure shows the zinc ion in site Zn1.[4] However, since the crystal structure of WT CphA was obtained from a crystal soaked in a solution containing a large excess of Zn^{2+} (10 mM), the presence of a single zinc ion in site Zn2 suggests that the monozinc species represents the native form of the B2 enzyme, CphA.

The N220G mutant structure

The refined structure of the mutant is essentially similar to that of the WT. The root-mean-square (r.m.s.) deviation between the C^{α} atoms of the two structures is 0.16 Å. Better-diffracting crystals allowed us to model the position of all 227 residues of the protein in the electron density map. Furthermore, the model contains one zinc ion, a carbonate ion located in the active site, three sulphate anions, two glycerol molecules, and 263 water molecules. The structure of the mutant shows two main features not seen in the structure of the WT enzyme. The first is that the N220G mutation leads to a localized conformational change in the protein backbone involving mainly residues Tyr218-Gly220 (Figure 3). In the WT structure, the last residue of β11, Tyr218, has backbone angles of φ = - 79° and ψ = 122°. Asn220 is the first residue of the 3_{10} helix, and Gly219 connects these two secondary structure elements. In the mutant structure, Gly220 increases the flexibility of the protein backbone, Tyr218 turns to φ= -114°, ψ = 133° and allows the Tyr218 hydroxyl group to form a hydrogen bond with the Val203 backbone nitrogen atom; two water molecules occupy the volume no longer occupied by the Asn220 side-chain. The second feature is a consequence of the previous one. The increased backbone mobility due to the N220G mutation alters the ability of Cys221 to coordinate the zinc ion. As a consequence, the zinc ion occupies two sites that are 1.5 Å apart, the WT site and the new site, with respective occupancies of 0.75 and 0.25 (Figure 2). In the new site, the zinc ion again presents a tetrahedral geometry with the Asp120-Cys221-His263 triad, but the fourth coordinating atom is NH2 of the buried Arg121. The distance between NH2 and the zinc in the new site is 2.3 Å and, surprisingly, the Arg121 side-chain seems to act as an electron donor for the zinc. Such coordination is unusual in proteins. To look for an example in small molecules, the Cambridge database[9] was searched, yielding the X-ray structure of a 1:1 complex between [(2-guanidinyl)ethyl-cyclen] and zinc, which is stable in aqueous solution at pH 7.5. In this small molecule complex, four nitrogen atoms of a cyclen ring and a nitrogen atom of guanidine in an imine form coordinate the zinc ion. In the WT and mutant CphA structures, the buried Arg121 side-chain makes several hydrogen bonds in the core of the protein with Glu69, Asn70, Tyr218, and Gly262 (Figure 3). Interestingly, in the mutant CphA structure, the buried Arg121 maintains all hydrogen bonds, whatever the position of the zinc. The guanidine group of the free arginine has a pK_a of around 12.5. The local environment inside the enzyme may significantly lower the pK_a value to generate the imine form of the guanidine group, which explains the observed coordination for zinc with a low occupancy.

The CphA-biapenem complex structure

Crystals of the CphA-biapenem complex were obtained by soaking crystals of the N220G mutant in mother liquor containing the antibiotic. The structure was solved by molecular replacement and, after refinement of all protein atoms, a difference electron density map ($|F_{complex}| - |F_{mutant}|$) was calculated,where $|F_{complex}|$ and $|F_{mutant}|$ are the structure factor amplitudes of the mutant crystal soaked in solution containing biapenem and of the mutant crystal alone, respectively). A well-defined electron density in the active site could not be interpreted as either a biapenem or a hydrolyzed biapenem molecule. The presence of two fused rings near the zinc ion was an unexpected finding (Figure 4). In order to shed light on this observation, substrate and product inhibition studies were initiated. The kinetic data clearly support the model of product inhibition with K_i values of 320 μM and 300 μM (±10%) for the WT and N220G enzymes, respectively. Both map interpretation and kinetic data agree with the presence of an intermediate in the hydrolysis reaction. The complex with the WT enzyme was prepared; however, the extra electron density in the active site was weaker, indicating a lower occupancy of the ligand bound to the enzyme. The refined CphA-biapenem complex structure comprises 227 protein residues, one zinc ion, six sulphate anions, and the intermediate molecule located in the groove of the active site with full occupancy. The r.m.s. deviation between the C^{α} atoms of the complex and mutant structures is 0.17 Å. Superimposition of the two structures shows that the binding of the intermediate induces a very localized

conformational change (G232-N233) in the active site (Figure 4). The intermediate is bonded to the zinc ion located at the WT position. The distance from the nitrogen atom of the β-lactam ring (N4) to the Zn^{2+} is 2.22 Å (Table 3). N4 also forms a hydrogen bond with Wat11 (2.9 Å) (Figure 5), which, in turn, forms hydrogen bonds with Asp120 and His118. The distance between Watll and the zinc atom is 3.39 Å. It was immediately clear from the first difference electron density map that the β-lactam ring had been cleaved between N4 and C7.

Furthermore, the map clearly indicated the presence of two free carboxyl groups in positions C3 and C7 (Figure 4).

Figure 3. *Stereo view of the active site of the N220G CphA mutant showing the backbone conformational change and the zinc coordination environment. The Y218-C221 residues of the wild-type CphA are coloured in magenta and superimposed for comparison. The two partially occupied positions of the zinc ion in the mutant are shown. The "natural" coordination position of zinc with occupancy 0.75 has D120, C221, H263, and a carbonate ion as ligands. The second coordination position with occupancy 0.25 has D120, C221, H263, and R121 as ligands. Water molecules referred to in the text and the hydrogen bond network in the active site are shown.*

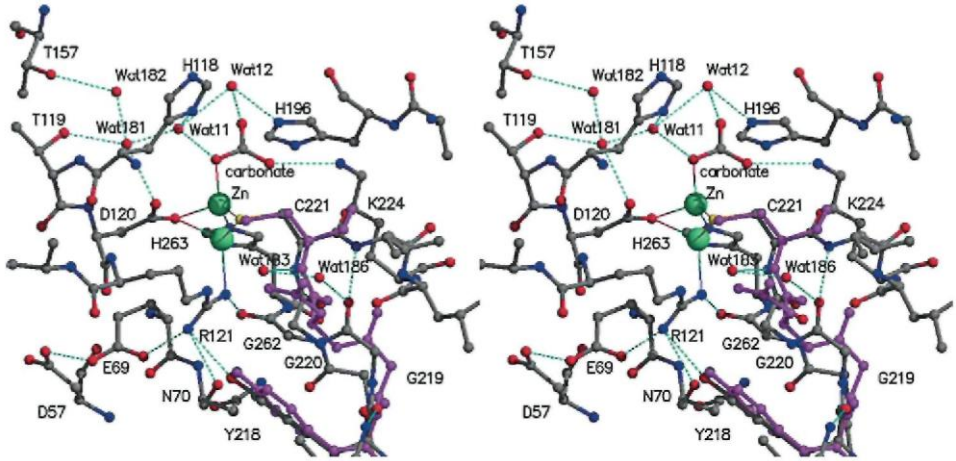

Table 3. *Interactions of the Zn ion and the intermediate with CphA*

Intermediate	CphA	Distance (Å)
Zn	D120 OD2	2.03
	C221 SG	2.27
	H263 NE2	2.12
	O32	2.39
	N4	2.22
N4	Wat11	2.9
	H263 NE2	2.9
	L224 NZ	3.1
O31	N233 NE2	3.1
	L224 NZ	2.9
	L224 NZ	2.9
O71	T119 OG1	3.1
	T157 OG1	2.9
O62	H196 NE2	3.0
	H196 NE2	3.0
S21	His263	3.6
Cl	W87 CH2	4.1
C62	N233 CB	3.8
	F236 CD2	3.7
	H118 CE1	4.2
C22	G232 CA	3.9
C25	V67 CG1	3.7
C29	V67 CG1	3.3
C25	H263 CG	4.0

Published in: Journal of Molecular Biology (2005), vol. 345, iss. 4, pp. 785-795.
Status: Postprint (Author's version)

Figure 4. *The F_o — F_c map (blue) at 2σ corresponding to the area of the complex structure where the enzyme-modified biapenem molecule was modelled. The phases were calculated from coordinates not completely refined without biapenem or solvent molecules in the active site. Final refined coordinates of modified biapenem, zinc, Wat11, D120, C221 and H263 residues have been superimposed.*

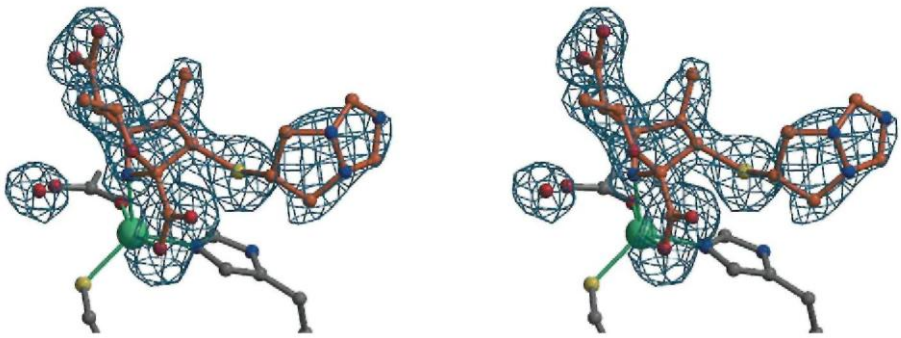

The C3 carboxyl group forms strong hydrogen bonds with the Lys224 side-chain nitrogen atom and the Asn233 backbone nitrogen atom. The C7 carboxyl group formed after antibiotic hydrolysis makes two hydrogen bonds with the two hydroxyl groups of Thr119 and Thr157. Surprisingly, both C2 and C3 of the intermediate exhibit sp^3 hybridization, showing that the molecule in the active site has lost the C2=C3 double bond. The side-chains containing the sulfur atom and the C3 carboxyl group are in the *cis* configuration. The biapenem is hydrolyzed and has lost the double bond, and it has undergone an internal molecular rearrangement. In fact, the electron density map shows a continuous density linking C3 to the oxygen atom of the C6 1-hydroxyethyl group, forming a six-membered ring fused to the hydrolyzed β-lactam ring (Figure 4). As the presence of a C2=C3 double bond and a C6 hydroxyethyl group are two main features of the carbapenem antibiotics currently in clinical use, we propose that a similar internal rearrangement may be common to all carbapenems. The intermediate in the active site is stabilized by several hydrophobic contacts. The biapenem sulfur atom interacts with the His263 ring, inducing a small rotation of its plane; the 1β-methyl group is in van der Waals contact with the side-chains of Trp87 and Val67, and the methyl group of the C6 1-hydroxyelthyl forms hydrophobic contacts with Phe156, Phe236 and the Asn233 side-chain carbon atom. In particular, the position of the Phe156 and Phe236 side-chains seems to preclude the possibility of having any bulkier group in C6 and retaining an efficient interaction between the intermediate and the enzyme. The biapenem σ-symmetric bicyclotriazoliumthio moiety is inserted between the Val67 side-chain and Gly232. Furthermore, its positively charged nitrogen atom interacts strongly with a water molecule located outside the active site (Figure 5).

Figure 5. *Stereo view of the active site of CphA in complex with modified biapenem (carbon atoms colored in orange). The conformational change upon substrate binding is represented by superimposition of the wild-type Gly232 and Asn233 residues (magenta).*

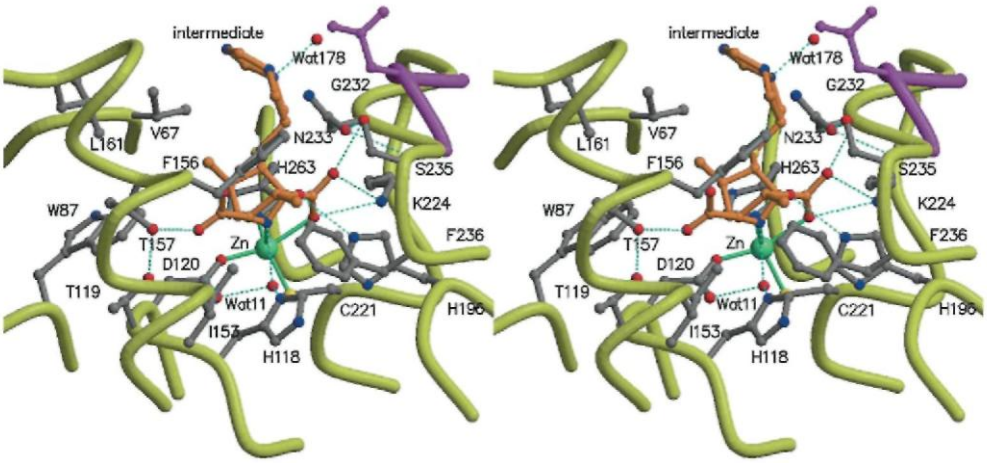

Published in: Journal of Molecular Biology (2005), vol. 345, iss. 4, pp. 785-795.
Status: Postprint (Author's version)

Figure 6. *The van der Waals surface of CphA in complex with modified biapenem (carbon atoms colored in orange). The zinc ion is represented as a green sphere.*

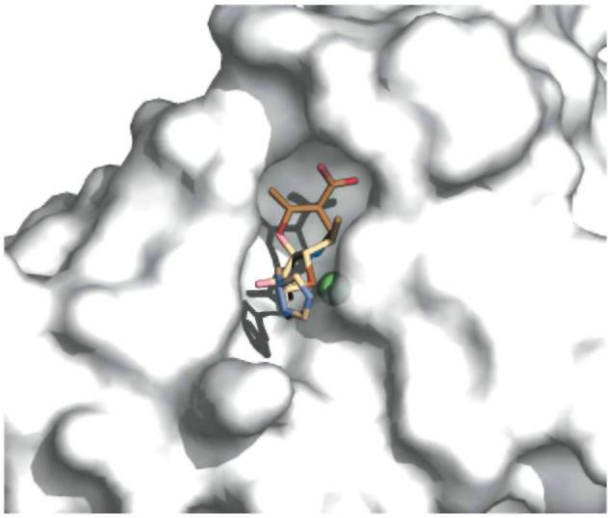

Upon biapenem binding, the Asn233 ψ angle changes from -18° to +121°, and this rotation orients the amide group of the Asn233 backbone towards the interior of the active site, allowing interaction with the C3 carboxyl group. As a result of the Asn233 side-chain rotation, the entrance to the active site is closed and Gly232 comes closer to the biapenem bicyclotriazoliumthio group. Furthermore, the Asn233 side-chain oxygen atom forms a hydrogen bond with the Ser235 hydroxyl group, stabilizing the closure of the loop. As a consequence, the "hydrophobic wall" from the N-domain and the mobile loop from the C-domain trap the antibiotic in the active site pocket, leaving only the terminal portion of the biapenem bicyclotriazoliumthio group outside the pocket (Figure 6). These interactions between the intermediate and the active site of the enzyme show that the active-site groove of CphA is designed perfectly for a carbapenem molecule.

Proposed reaction pathway

Comparison of the three new structures suggests how subclass B2 metallo-β-lactamases recognize carbapenem antibiotics and allows detailed mechanistic proposals for antibiotic hydrolysis (Figure 7). In the resting state, the enzyme has a carbonate ion at its active site (Figure 3), bonded to the positively charged zinc ion and the Lys224 side-chain. The Gly232-Asn233 loop located at the entrance of the active site that has been implicated in substrate binding is in the open position. The side-chains of His118 and His196, which are ligands of Zn1 site, are involved in a hydrogen bond network with water molecules and appear to aid in holding the carbonate ion in place. A carbonate ion was found in the *B. cereus* metallo-β-lactamase structure (PDB code 1BVT) and in leucyl amino-peptidase (PDB code 1LAM), another zinc hydrolase. For the CphA enzyme, the inhibition constant is rather high (K_D 13(± 2) mM), suggesting no physiological role for the carbonate ion. In the structure of the CphA-biapenem complex, eight hydrogen bonds between the carbapenem molecule and the protein as well as two bonds with the zinc ion are observed (Figure 7e and Table 3). The former involve the side-chains of Thr119, Thr157, His196, and Lys224, the nitrogen backbone of Asn233, and Wat11. Intermediate structures (Figure 7a-d) were modeled on the basis of the X-ray structures of native and biapenem-complexed proteins, allowing only a rotation of side-chains (Figure 7b). The presence of a carbapenem molecule in the active site leads to the closure of the external loop, trapping the antibiotic. In the structure of the complex (Figure 7e), the C3 carboxyl group makes a bond with the zinc ion, and interacts with the NH_3^+ of Lys224, and the Asn233 nitrogen backbone, the last of which is brought into the correct orientation by the loop closure. Thr119 and Thr157 form hydrogen bonds with, and Phe156 and Phe236 form hydrophobic interactions with, the hydro-xyethyl group, which helps to stabilize and orient the antibiotic molecule. Substrate binding promotes the polarization of the β-lactam ring carbonyl oxygen atom by His196 (Figure 7a). The Asn116 side-chain nitrogen atom and the Thr197 hydroxyl group form hydrogen bonds with the His196 side-chain nitrogen atom. This hydrogen bonding network allows His196 to partially donate its hydrogen atom to the β-lactam ring carbonyl oxygen atom. A water molecule, activated by His118, attacks the carbonyl carbon atom and cleaves the β-lactam bond. As a consequence, N4 of carbapenem bonds to the zinc ion. The Zn^{2+} also helps in the correct orientation of the β-lactam ring during hydrolysis (Figure 7b and c).

Published in: Journal of Molecular Biology (2005), vol. 345, iss. 4, pp. 785-795.
Status: Postprint (Author's version)

Figure 7. *Scheme of the proposed mechanism of β-lactam hydrolysis by CphA, as deduced from the structures described here.*

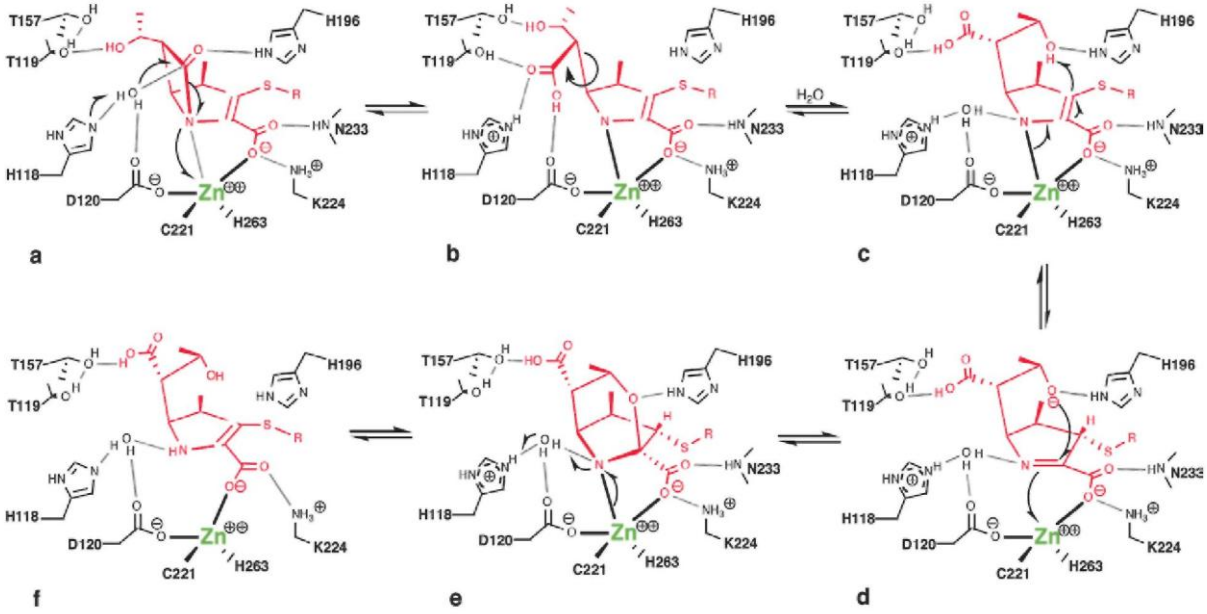

The carboxyl group generated by the hydrolytic process is stabilized initially by His196, Asp120, and His118 (Figure 7b) but, after rotation around the C5-C6 bond, these interactions are replaced by those observed in the complex (Figure 7c) between the carboxyl group and Thr119, Thr157. Interestingly, the incoming water molecule (Watll) is located in a position suitable for promoting the protonation of the lactam nitrogen atom, which will weaken the interactions with the zinc ion (Figure 7c). At the last step of the catalytic reaction (Figure 7f), the hydrolyzed carbapenem molecule can leave the active site. Finally a shorter pathway is possible between the intermediate (Figure 7c) and the product models (Figure 7f). However, in the present experimental conditions, the kinetic parameters support the longer one. The tautomeriza-tion between an enamine and an imine form of the β-lactam ring allows the transfer of a proton from the hydroxyethyl group OH to C2, followed immediately by nucleophilic attack on C3 by the oxygen atom of the same side-chain. The presence of the carboxylate group will render the imine group electron-deficient, promoting nucleophilic addition. The cyclization process appears to be supported strongly by the proximity of the Zn^{2+} (Figure 7d). Another interesting observation is that the active site of CphA is fully occupied by the intermediate (Figure 6), leaving no space for further water molecules in the proximity of Wat11, the closest being the buried Wat43, which forms hydrogen bonds with His196, Asn116, and Thr197. The position of Wat43 suggests a possible way of access of water molecules to the zinc catalytic center during hydrolysis.

Discussion

Here, we report the first structures for a member of metallo-β-lactamase subclass B2 in both the native and mutant forms and in the form of a complex with an intermediate generated during hydrolysis of a carbapenem antibiotic. The overall general architecture of CphA is similar to that of enzymes of the other subclasses. However, it has an elongated helix (α3) located just above the active-site pocket. The α3 helix is a key element of the hydrophobic wall that defines the active-site pocket. In subclass B1, there is a long loop between β2 and β3, which is disordered in the native structure, but is stabilized upon binding of inhibitor.[11] This long loop is missing from subclasses B2 and B3. However, compared to subclass B2, subclass B3 enzymes have a shorter insertion between α3 and β7, also forming a mobile loop near the active site. Consequently, in CphA, we observe a very well defined active site, which explains the very narrow activity profile of the enzyme. CphA is mononuclear, the zinc ion being located in the Zn2 site, whereas, in all other structures known, two zinc ions can be bound and, if a functional monozinc enzyme can be produced in the native form, the zinc ion is located in the Zn1 site. In CphA, as hypothesized, even in the presence of a large excess of zinc, ligands in positions 116, 118, and 196 (Zn1 site) do not interact with any zinc ion. Instead, Asn116, His118, and His196, together with Lys224, form a hydrogen bond network in the active site involving several water molecules. This could be due to the His116Asn mutation seen in subclass B2. GOB-1, a subclass B3 enzyme, harbors Gln116 and may therefore be a monozinc enzyme. Finally, an excess of zinc results in a loss of enzymatic activity. Although the dissociation constant of the second zinc ion is about 50 μM, we did not observe the binding of a second zinc ion, even at a

very high concentration of zinc in the mother liquor. This apparent discrepancy might result from the presence of a carbonate ion in the active site and/or the conditions used to grow crystals. Indeed, the residues in the putative Znl site are not positioned adequately to bind Zn in the native enzyme and solution NMR measurements indicate major conformation changes upon binding of the second zinc ion (C. Damblon, personal communication).

Attempts to obtain substrate complexes or convincing information about modes of substrate binding using docking procedures have always failed for B1 and B3 enzymes.[7,11,13] Recently an interesting report was published on simulations of substrate binding to the mononuclear *B. cereus* metallo-β-lactamase.[14] Using a high concentration of substrate in the crystallization drop, we succeeded in trapping an intermediate filling the narrow active-site pocket of CphA. Previous failures with subclass B1 and B3 enzymes could be due to the presence of a long active-site cleft covered by a mobile loop.

In metallo-β-lactamases containing two zinc ions, the catalytic mechanism of β-lactam hydrolysis has been proposed to involve a bridging hydroxide group located between the two zinc ions, which can serve as the attacking nucleophile on the carbonyl oxygen atom of the β-lactam ring.[5,7,15] In this mechanism, Znl would polarize the carbonyl oxygen atom. However, it has been suggested that under physiological conditions and in the presence of substrate, metallo-β-lactamases would act as monozinc enzymes,[2] but it is not known whether the zinc is in the Zn1 or the Zn2 site or partially in both. For the CphA enzyme, the dissociation constants for the binding of zinc ions in the presence or absence of substrate are 1.2 pM and 7.0 pM, respectively[2] and the present structures show that the zinc ion is located in the Zn2 site. These results support earlier finding demonstrating a full occupancy of a single zinc ion with a Cys sulphur atom as a ligand.[3,16] So, for the first time in the metallo-β-lactamase family, we have determined the structure of the enzyme as it is under the expected physiological conditions. The first reported structure of the family reveals a monozinc enzyme with the ion located in the Zn1 site. On the basis of the observed active-site geometry, a catalytic mechanism was proposed by analogy to the zinc peptidases,[4] in which the zinc ion has a dual role in catalysis. Firstly, a zinc-bound water molecule is activated to perform a nucleophilic attack on the β-lactam carbonyl group. Secondly, the zinc ion binds and polarizes this carbonyl group. Asp120 participates in the activation of the water molecule. A more recent publication analyses the proposed catalytic mechanism on the basis of the pH-dependence of the hydrolysis rate and kinetic constants.[17] This mechanism and our proposed mechanism for CphA are completely different. However, since the active sites of the *B. cereus* and CphA enzymes are quite different, it is reasonable to hypothesize that the β-lactam hydrolysis proceeds according to different mechanisms in the two enzymes.

In conclusion, the three reported structures reveal one molecular mechanism of β-lactam hydrolysis by subclass B2 metallo-β-lactamases and may help in designing small molecules for specific therapeutic applications.

Materials and Methods

Protein purification and crystallization

Site-directed mutagenesis, protein expression at 18 °C and purification of the proteins were performed as described.[18] The purified enzyme solution was dialyzed against 15 mM sodium cacodylate (pH 6.5). As measured by inductively coupled plasma-mass spectrometry (ICP-MS), the WT and mutant enzyme contained one zinc ion per molecule. Initial screening experiments were performed by a TECAN Genesis robot using commercial Hampton crystallization screens. N220G CphA (~10mg ml^{-1}) was crystallized at 8 °C from 30-34% (w/v) PEG8000, 0.6-0.8 M ammonium sulphate, and 100 mM sodium citrate (pH 6.5), using the hanging-drop method. The (2 µl) reservoir solution was mixed with the protein solution (2 µl) and the mixture was left to equilibrate against the reservoir solution. Typically, crystals grew within a few days to dimensions of 80 µm x l00 µm x l00 µm. Crystals of the WT protein were obtained under similar crystallization conditions using mutant micro-crystals as starting seeds. Before data collection, both the WT and the mutant crystals were transferred to drops of reservoir solution containing 10 mM $ZnCl_2$ and soaked for one day. In order to obtain the mercury derivative, crystals of the mutant were instead washed using the reservoir solution for removing the excess of $ZnCl_2$, and transferred to a drop of reservoir solution containing 1 mM sodium *p*-hydroxy-mercurio-benzoate. The biapenem-CphA complex was obtained by adding an excess of biapenem powder directly to a drop containing mutant CphA crystals.

Data collection and processing

A mercury derivative crystal was transferred to cryoprotectant solution (reservoir solution containing 20% (v/v) glycerol), while WT and mutant crystals were transferred to cryoprotectant solution containing 10 mM $ZnCl_2$, then the crystals were mounted rapidly in loops and flash-cooled. X-ray data for the WT and for the mutant CphAs were collected at the European Synchrotron Radiation Facility at the BM30A beam-line. X-ray data for the biapenem-CphA complex were obtained in-house using a Nonius FR591 rotating anode X-ray generator coupled to a Mar Research Imagine Plate detector. Data were processed using CCP4 programs (MOSFLM and SCALA)[19] (Table 2).

Structure determination and refinement

The structure of mutant CphA was solved using the single isomorphous replacement with anomalous scattering (SIRAS) method, in which phases to 1.7 Å were generated using data from the inflection and peak of the mercuric derivative and data from the mutant. One mercury atom was located in the asymmetric unit using SOLVE.[20] Phase refinement resulted in a figure of merit (FOM) of 0.60 and yielded a partially interpretable map. Density modification and automatic building using RESOLVE[21] resulted in a model that included 81% of the sequence. Multiple rounds of model building with O[22] and refinement with REFMAC gave the final structure. The crystals of native and complexed CphA were isomorphous with the mutant crystals. Initial phases for the native and complexed structures were obtained using the structure of the mutant as the starting model. Refinement was carried out using O and REFMAC. For the complex, the calculation of the first (F_o—F_c) electron density map clearly showed the presence of the antibiotic molecule in the active site. Biapenem was modeled in the map after most of the protein main-chain and side-chain atoms and most of the water molecules were built and refined. Conformational torsion angle restraints and charge assignments for the intermediate molecule were obtained using CCP4i Libcheck. The refinement statistics for all structures are shown in Table 2.

Enzyme kinetics

Kinetic parameters were determined routinely on the basis of initial rate measurements at 30 °C and in 15 mM sodium cacodylate (pH 6.5). Absorbance variations were monitored at 300 nm ($\Delta\varepsilon$= -9000 M^{-1} cm^{-1}) and 294 nm ($\Delta\varepsilon$ = -9960 M^{-1} cm^{-1}) for imipenem and biapenem, respectively. Substrate concentrations ranged from 0.5 K_m to 2 K_m. Above 250 µM, a 0.2 cm light-path cell was utilized.

Product inhibition determination

The kinetic parameters of the enzymes with biapenem as substrate were determined on the basis of both complete time-courses and initial rates. For both the WT and the mutant enzymes, the k_{cat} and K_m values were significantly lower according to the latter technique. This suggested an inhibition by the product.[23] Indeed, after biapenem solutions were hydrolyzed completely, addition of a fresh substrate sample yielded initial rates lower than the original ones.

Protein Data Bank accession codes

Coordinates and structure factors have been deposited with the Protein Data Bank using accession codes 1X8G (wild-type), 1X8H (N220G mutant), and 1X8I (biapenem complex).

Acknowledgements

We are grateful to Richard Kahn for assistance in data collection at the BM30A beam-line at the European Synchrotron Radiation Facility, Grenoble, France. G.G. is a recipient of a postdoctoral fellowship from the European Union in the frame of the MEBEL contract (HPRN-CT-2002-00264). The work in Liège was supported by a grant from the Belgian Federal Government (PAI P5/33) and the FNRS (Brussels, Belgium, FRFC contract 2.4508.01). C.B. is a pre-doctoral fellow of the FRIA (Brussels) and C.A. was a recipient of a Marie Curie Postdoctoral fellowship (Human Potential-grant IHM-MCIF-01-1).

References

1. Garau, G., Garcia-Saez, I., Bebrone, C., Anne, C., Mercuri, P., Galleni, M. *et al.* (2004). Update of the standard numbering scheme for class B beta-lactamases. *Antimicrob. Agents Chemother.* 48, 2347-2349.

2. Wommer, S., Rival, S., Heinz, U., Galleni, M., Frère, J. M., Franceschini, N. *et al.* (2002). Substrate-activated zinc binding of metallo-beta-lactamases: physiological importance of mononuclear enzymes, *J. Biol. Chem.* 277, 24142-24147.

3. Hernandez-Valladares, M., Felici, A., Weber, G., Adolph, H. W., Zeppezauer, M., Rossolini, G. M. *et al.* (1997). Zn(II) dependence of the *Aeromonas hydrophila* AE036 metallo-beta-lactamase activity and stability. *Biochemistry,* 36, 11534-11541.

4. Carfi, A., Parès, S., Duée, E., Galleni, M., Duez, C., Frère, J. M. *et al.* (1995). The 3-D structure of a zinc metallo-beta-lactamase from *Bacillus cereus* reveals a new type of protein fold. *EMBO J.* 14, 4914-4921.

5. Concha, N. O., Rasmussen, B. A., Bush, K. & Herzberg, O. (1996). Crystal structure of the wide-spectrum binuclear zinc β-lactamase from *Bacteroides fragilis. Structure,* 4, 823-836.

6. Fabiane, S. M., Sohi, M. K., Wan, T., Payne, D. J., Bateson, J. H., Mitchell, T. *et al.* (1998). Crystal structure of the zinc-dependent beta-lactamase from *Bacillus cereus* at 1.9 Å resolution: binuclear active site with features of a mononuclear enzyme. *Biochemistry,* 37, 12404-12411.

7. Ullah, J. H., Walsh, T. R., Taylor, I. A., Emery, D. C., Verma, C. S., Gamblin, S. J. *et al.* (1998). The crystal structure of the L1 metallo-beta-lactamase from *Stenotrophomonas maltophilia* at 1.7 Å resolution. *J. Mol. Biol.* 284, 125-136.

8. Garcia-Sáez, I., Mercuri, P. S., Papamicael, C., Kahn, R., Frère, J.-M., Galleni, M. *et al.* (2003). Three-dimensional structure of FEZ-1, a monomeric subclass B3 metallo-beta-lactamase from *Fluoribacter gormanii,* in native form and in complex with D-captopril. *J. Mol. Biol.* 325, 651-660.

9. Allen, F. H. (2002). The Cambridge structural database: a quarter of a million crystal structures and rising. *Acta Crystallog. sect. B,* 58, 380-388.

10. Aoki, S., Iwaida, K., Hanamoto, N., Shiro, M. & Kimura, E. (2002). Guanidine is a Zn(2+)-binding ligand at neutral pH in aqueous solution, *J. Am. Chem. Soc.* 124, 5256-5257.

11. Garcia-Sáez, I., Hopkins, J., Papamicael, C., Franceschini, N., Amicosante, G., Rossolini, G. M. *et al.* (2003). The 1.5-Å structure of *Chryseobacterium meningosepticum* zinc β-lactamase in complex with the inhibitor, D-captopril. *J. Biol. Chem.* 278, 23868-23873.

12. Hernandez-Valladares, M., Kiefer, M., Heinz, U., Meyer-Klaucke, R., Nolting, W., Paul Soto, H. F. *et al.* (2000). Kinetic and spectroscopic characterization of native and metal- substituted beta-lactamase from *Aeromonas hydrophila* AE036. *FEBS Letters*, 467, 221-225.

13. Concha, N. O., Janson, C. A., Rowling, P., Pearson, S., Cheever, C. A., Clarke, B. P. *et al.* (2000). Crystal structure of the IMP-1 metallo beta-lactamase from *Pseudomonas aeruginosa* and its complex with a mercaptocarboxylate inhibitor: binding determinants of a potent, broad-spectrum inhibitor. *Biochemistry*, 39, 4288-4298.

14. Dal Peraro, M., Vila, A. J. & Carloni, P. (2004). Substrate binding to mononuclear metallo-beta-lactamase from *Bacillus cereus. Proteins: Struct. Funct. Genet.* 54, 412-423.

15. Wang, Z., Fast, W., Valentine, A. M. & Benkovic, S. J. (1999). Metallo-beta-lactamase: structure and mechanism. *Curr. Opin. Chem. Biol*. 3, 614-622.

16. Meyer-Klaucke, W., Soto, R. P., Valladares, M. H., Adolph, H. W., Nolting, H. E., Frère, J.-M. *et al.* (1999). A comparison of *Bacillus cereus* and *Aeromonas hydrophila* Zn-beta-lactamases. *J. Synchrotron Radiat.* 6, 400-402.

17. Bounaga, S., Laws, A. P., Galleni, M. & Page, M. I. (1998). The mechanism of catalysis and the inhibition of the *Bacillus cereus* zinc-dependent beta-lactamase. *Biochem. J.* 331, 703-711.

18. Vanhove, M., Zakhem, M., Devreese, B., Franceschini, N., Anne, C, Bebrone, C. *et al.* (2003). Role of Cys221 and Asnll6 in the zinc-binding sites of the *Aeromonas hydrophila* metallo-beta-lactamase. *Cell Mol. Life Sci.* 60, 2501-2509.

19. The CCP4. (1994). CCP4 suite: programs for protein crystallography. *Acta Crystallog. sect. D,* 50, 760-763.

20. Terwilliger, T. C. & Berendzen, J. (1999). Automated MAD and MIR structure solution. *Acta Crystallog. sect.* D, 55, 849-861.

21. Terwilliger, T. C. & Berendzen, J. (2000). Maximum-likelihood density modification. Automated MAD and MIR structure solution. *Acta Crystallog. sect. D,* 56, 965-972.

22. Jones, T. A., Zou, J.-Y., Cowan, S. W. & Kjeldgaard, M. (1991). Improved methods for building protein models in electron density maps and the location of errors in these models. *Acta Crystallog. sect. A,* 47, 110-119.

23. Orsi, B. A. & Tipton, K. F. (1979). Kinetic analysis of progress curves. *Methods Enzymol.* 63, 159-183.